Density-functional study of bulk and surface properties of titanium nitride using different exchange-correlation functionals

M. Marlo
Laboratory of Physics, Helsinki University of Technology, P.O. Box 1100 FIN-02015 HUT, Finland

V. Milman
Molecular Simulations Inc., The Quorum, Barnwell Road, Cambridge CB5 8RE, United Kingdom
(Received 31 January 2000)

The adsorption and diffusion of hydrogen on the (100) surface of titanium nitride was studied using density-functional theory (DFT) and the generalized gradient approximation (GGA) for the exchange and correlation energy. The adsorption site was found to be on top of the titanium atom with the chemisorption energy of -2.88 eV. The diffusion barrier was determined as 0.73 eV along the path connecting the neighboring titanium atoms. The surface energies and surface relaxations of the three most important surfaces of TiN were studied. The surface energies have the following order: $S_{100}<S_{110}<S_{111}$. Three different GGA functionals, the Perdew-Wang 1991 (PW91), the Perdew-Burke-Ernzerhof (PBE), and the revised PBE (RPBE) functionals, were tested on crystals, small molecules and TiN surfaces. The RPBE functional when applied to the surface studies of TiN was found to produce slightly lower values of surface energies and of hydrogen adsorption energies than the PW91 functional.

I. INTRODUCTION

Titanium nitride is a metallic compound characterized by high melting point, ultra-hardness (comparable to that of diamond), good electrical and thermal conductivity, and high resistance to corrosion.[1] Because of its superior properties TiN is widely used in various industrial applications. The exceptional hardness and wear resistance enable the use of TiN as a high-performance coating material. TiN has also become attractive in silicon microelectronics technology due to its excellent diffusion barrier characteristics, very good electrical conductivity, and excellent adhesion/glue layer performance.[2,3] There is a large body of experimental work devoted to various aspects of titanium nitride film growth.[2–5] However, no atomistic studies of TiN films nor TiN surfaces exist, although the performance of TiN films was found to be dependent on the surface structure and orientation.[3–8]

TiN belongs to a class of refractory metals where a nonmetallic element (N, C, or O) forms a compound with a transition-metal element. The unusual combination of metal and nonmetal and interesting properties of refractory compounds have challenged scientists to explain the nature of bonding in these materials. The studies of the properties of bulk TiN are quite rare despite the great industrial interest in this material. The band structure calculations for TiN and other refractory metals were presented in Ref. 1. The charge density distribution and the nature of bonding in TiN and TiC were investigated using the linearized-augmented-plane-wave (LAPW) method[9] and the results were found to compare well with the data obtained with x-ray-diffraction studies.[10] The lattice constant and bulk modulus of TiN were obtained theoretically by the full-potential linear muffin-tin-orbital (FP LMTO) method in Ref. 11.

Titanium nitride films are usually produced by various chemical vapor deposition (CVD) techniques[2,3,5,12,13] although sputtering[4,6] and ion beam processing[7] have been also used to grow TiN films. However, the CVD approach has been adopted as a preferred deposition technique in industrial applications. A typical CVD procedure would use as reactants such gas mixtures as $TiCl_4$ and NH_3,[3] TiI_4 and NH_3,[13] $TiCl_4$-NH_3-H_2,[12] $TiCl_4$-NH_3 with organic additives,[2] etc. Theoretical calculations of the binding energies and diffusion barriers for various atoms, molecules, and fragments involved in the growth process could provide specific information on atomic processes on the surface that is required for quantitative modeling of CVD reactors.[14,15] Related information on surface energies and surface structures can help to interpret the growth processes.

The purpose of the present study was to investigate the three surfaces most commonly observed in the growth processes and to model adsorption and diffusion of atomic hydrogen on the most stable clean surface of TiN. Bulk properties of TiN such as the lattice constant, bulk modulus B, its pressure derivative B', and elastic constant tensor were calculated as well.

Density-functional theory (DFT) and the local-density approximation (LDA) have become a widely accepted scheme for studying electronic ground state properties of solids, surfaces, and molecules.[16] The development of nonlocal exchange and correlation functionals has demonstrated that the bond energies of molecules, the cohesive energies of solids, and the energy barriers of molecular reactions can be greatly improved compared to the LDA results.

Recently there have been numerous suggestions for the functional form of the generalized gradient approximation (GGA). The most frequently used form is the Perdew-Wang[17] 1991 (PW91) functional, which has been applied to a variety of problems in physics and chemistry of solids and surfaces. Perdew, Burke, and Ernzerhof[18] (PBE) constructed a simpler functional form than the traditional PW91 functional. The PBE functional is designed to reproduce closely the PW91 results, although the PBE formulation is intended to be more robust. The RPBE functional[19] repre-

sents a minor revision of the PBE form, where the difference is only in the functional form of the exchange enhancement factor.

The RPBE functional improves significantly the accuracy of calculated chemisorption energies of small molecules on metal surfaces. The RPBE approach has been tested exclusively on small molecules in a gas phase[19] and on adsorption energies of atomic and molecular species on metallic surfaces.[19–22] It has become customary[20–22] to apply RPBE to calculations of total energies based on the structure and electron density obtained with the PW91 functional. This procedure seems to be arbitrary and it is unsuitable for predictive studies of material properties. It would be preferable to use the same exchange-correlation functional throughout, providing that it describes the ground state properties with sufficient accuracy.

The aim of this paper is to present a theoretical study of the surface properties of TiN, including an investigation of the hydrogen adsorption on the surface. It appears that an additional testing of GGA functionals was needed to be able to use the RPBE approach with confidence. In view of this situation we tested three GGA functionals, namely, PW91, PBE, and RPBE, by calculating ground state properties of a few crystals and small molecules, as well as by applying these functionals to the surface calculations for TiN. The RPBE functional appears to be sufficiently accurate in these tests, so we carried out the study of hydrogen adsorption on the (100) surface of TiN using this functional. We also calculated chemisorption energies of H on TiN with the PW91 and RPBE functionals in order to get further information on the performance of the rather new functional (RPBE) in comparison to other GGA functionals.

This work is organized as follows. In Sec. II we describe the approach used and present the results. In Sec. II A we briefly discuss the computational details. In Sec. II B we compare the results obtained with the three GGA functionals, PW91, PBE and RPBE, for six crystals and for three small molecules. The results for bulk TiN and for three TiN surfaces are presented in Sec. II C, and in Sec. II D we examine the diffusion and adsorption of atomic hydrogen on the (100) surface of TiN. Preliminary results of the study of dissociative adsorption of H_2 molecule on the (100) surface of TiN are given in Sec. II E. In Sec. III we summarize the findings of the comparative testing of GGA functionals and then discuss the results related to the growth of titanium nitride films.

II. SIMULATIONS AND RESULTS

A. Computational details

DFT GGA simulations were performed using computer program CASTEP (Cambridge Serial Total Energy Package).[23] CASTEP is a DFT-based pseudopotential package, where a plane wave basis set is used for expanding electronic states. In order to reduce the number of plane waves required, chemically inactive core electrons are effectively replaced with ultrasoft pseudopotentials,[24,25] which in this work were taken from the CASTEP database.[23] Two parameters that affect the accuracy of calculations are the kinetic energy cutoff, which determines the number of plane waves in the expansion and the number of special k points used for the Brillouin zone integration (see Ref. 16 for details).

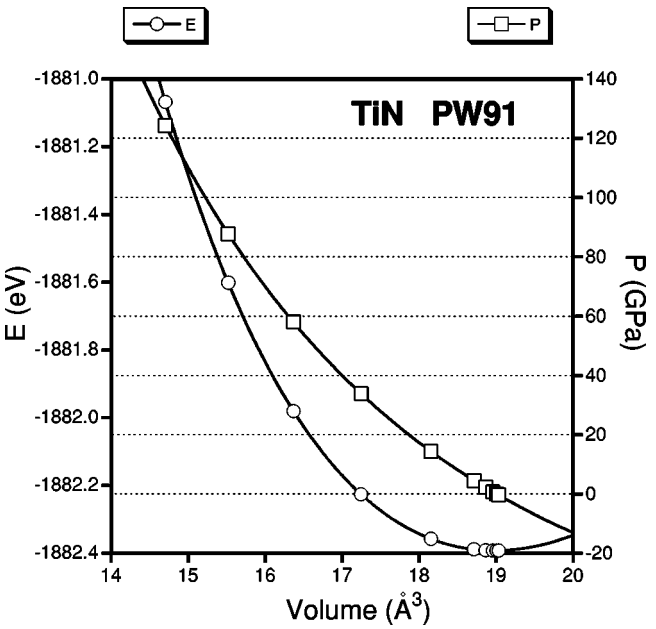

FIG. 1. Equation of state for TiN calculated with the PW91 functional.

The density mixing scheme based on the Pulay algorithm is used to find the electronic ground state.[23,25] Thermal smearing of one-electron states ($k_BT=0.1$ eV) was used to converge calculations for metallic systems.[23]

B. Testing of GGA functionals

1. Crystals

We studied six different materials with three GGA functionals. The lattice constant, bulk modulus, and its pressure derivative were obtained by calculating the total energy and pressure for different values of the unit cell volume and by fitting the calculated data to the third-order Birch-Murnaghan equation of state (EOS):[26]

$$p(V)=\frac{3}{2}B\left[\left(\frac{V_0}{V}\right)^{7/3}-\left(\frac{V_0}{V}\right)^{5/3}\right]\times\left\{1+\frac{3}{4}(B'-4)\left[\left(\frac{V_0}{V}\right)^{2/3}-1\right]\right\}, \qquad (2.1)$$

where V_0 is the unit-cell volume at zero pressure, B is the bulk modulus, and B' is the pressure derivative of the bulk modulus at zero pressure. The energy and pressure dependence of the volume for TiN calculated with PW91 is shown in Fig. 1. Errors from the numerical fitting were less than 1 GPa for the bulk modulus and less than 0.2 for B' in all materials. The error bars were significantly smaller, around 0.1 GPa, for softer materials with small values of B. The calculated equilibrium lattice constants, bulk moduli, and their pressure derivatives are given in Table I. In addition to the results obtained with three GGA functionals, we present the LDA result for TiN.

PBE and PW91 give very similar results in all materials and for all calculated properties. In metals (Al, TiN) and

TABLE I. Lattice constant and its percentage deviation from the experimental value, bulk modulus, and its pressure derivative calculated with different exchange-correlation functionals.

		a_0 (Å)	Error	B (GPa)	B'
Al	Expt.	4.05[a]		79[b]	4.2[c]
	PW91	3.955	−2.3%	85	4.8
	PBE	3.954	−2.4%	86	4.7
	RPBE	3.952	−2.4%	87	4.5
TiN	Expt.	4.238[d]		288[e]	
	LDA	4.175	−1.5%	319	4.3
	PW91	4.236	−0.0%	282	4.2
	PBE	4.237	−0.0%	282	4.2
	RPBE	4.260	+0.5%	266	4.2
Ge	Expt.	5.66[a]		75[f]	
	PW91	5.547	−2.0%	76	4.7
	PBE	5.550	−1.9%	75	4.7
	RPBE	5.558	−1.8%	73	4.8
C (diamond)	Expt.	3.567[g]		442[g]	4.0[g]
	PW91	3.534	−0.9%	450	3.2
	PBE	3.533	−1.0%	450	3.3
	RPBE	3.537	−0.8%	445	3.3
MgO	Expt.	4.21[a]		163[h]	4.0[h]
	PW91	4.275	+1.5%	145	4.5
	PBE	4.277	+1.6%	143	4.6
	RPBE	4.314	+2.5%	134	4.5
NaCl	Expt.	5.598[i]		24[j]	5.4[k]
	PW91	5.682	+1.5%	29	4.6
	PBE	5.686	+1.6%	24	4.6
	RPBE	5.828	+4.1%	20	4.5

[a]Reference 27.
[b]Reference 28.
[c]Reference 29.
[d]Reference 30.
[e]Reference 31.
[f]Reference 32.
[g]Reference 33.
[h]Reference 34.
[i]Reference 35.
[j]Reference 36.
[k]Reference 37.

covalent crystals (Ge, C) the RPBE functional seems to produce the values for lattice constant that are similar to those obtained using PBE and PW91 functionals, but in ionic crystals RPBE gives a somewhat larger lattice constant. This rather limited study seems to suggest that a clearly ionic character of bonding, such as in NaCl, results in a larger difference between the results obtained with different GGA functionals than the moderately ionic character, as in MgO. In all materials, except in Al where the differences between the results obtained with different GGA functionals are negligible, the RPBE functional gives larger values for the lattice constant and smaller values for the bulk moduli than the PBE and PW91 functionals. On the other hand, the PBE and PW91 functionals yield essentially identical results in all cases.

2. Molecules

We studied three small molecules, CO, Cl_2, and O_2 with spin-dependent GGA functionals (GGS). We have listed molecular bond lengths and corresponding experimental values in Table II.

TABLE II. Calculated bond lengths of small molecules obtained using different GGA functionals in comparison with experimental values.

		a (Å)	Error
CO	Expt.	1.128[a]	
	GGS PW91	1.143	+1.3%
	GGS PBE	1.144	+1.4%
	GGS RPBE	1.144	+1.4%
Cl_2	Expt.	1.988[a]	
	GGS PW91	1.978	−0.5%
	GGS PBE	1.972	−0.8%
	GGS RPBE	1.979	−0.4%
O_2	Expt.	1.217[a]	
	GGS PW91	1.230	+1.1%
	GGS PBE	1.232	+1.2%
	GGS RPBE	1.233	+1.3%

[a]Reference 38.

RPBE gives the largest value for the molecular bond length, which is consistent with the overestimated lattice parameters in solids. The differences between the three functionals are, however, very small, of the order of milliångstroms. In summary, the properties of materials with little or no charge transfer are described by the RPBE functional with approximately the same accuracy as that of PBE or PW91 functionals.

C. Calculations on TiN and TiN surfaces

1. Titanium nitride

The lattice constant, bulk modulus, and its pressure derivative for TiN are given in Table I. We calculated these values with three GGA functionals and using the LDA. The LDA resulted in a smaller value for the lattice constant and a larger bulk modulus in comparison to GGA. It appears that the GGA describes titanium nitride properties better than the LDA. The PW91 and PBE results are in particularly good agreement with experimental values. Earlier all-electron FP-LMTO calculations for TiN in Ref. 11 gave results that are very similar to those quoted in Table I. The lattice constant and bulk modulus were reported as 4.161 Å and 310 GPa within the LDA, and 4.230 Å and 270 GPa within the PW91 GGA. In that work both lattice constants and bulk moduli were slightly smaller than ours.

It is worth noting that the experimental value of $B=318$ GPa, quoted in Ref. 11, seems to be less reliable than the value we used, 288 GPa, as taken from Ref. 31. The latter value comes from bulk tests and agrees well with another bulk result, 292 GPa, as given in Ref. 39. The higher value quoted in Ref. 11 is taken from the experimental study[40] that derived elastic constants from the slope of the dispersion curves of surface phonons on TiN films. Two factors suggest that the lower value of 288 GPa is the reliable one, namely, the difference between the bulk and thin film elastic properties and the difference between the static and dynamic bulk modulus.

The full elastic constant tensor calculated with three GGA functionals (PW91, PBE, RPBE) and using LDA is pre-

TABLE III. Elastic constants for titanium nitride (GPa). Present results are compared to the previous FP LMTO calculations (Ref. 11) and to the available experimental data. B_{EOS} is the bulk modulus obtained from the EOS fitting, $B=(C_{11}+2C_{12})/3$, $C'=(C_{11}-C_{12})/2$.

	C_{11}	C_{12}	C_{44}	C'	B	B_{EOS}
PW91	600	120	159	240	280	282
PW91[a]	610	100	168	255	270	
PBE	598	118	159	240	278	282
RPBE	561	116	156	223	265	266
LDA	704	125	168	290	318	319
LDA[a]	735	93	250	321	307	
Expt.[b]	625	165	163	230	318	
Expt.[c]						288
Expt.[d]						292

[a]Reference 11.
[b]Reference 40.
[c]Reference 31.
[d]Reference 39.

sented in Table III. Our results are in reasonable agreement with the values obtained from the all-electron calculations.[11] Internal consistency of the calculation is demonstrated by the fact that the bulk modulus obtained by fitting an analytical equation of state agrees well with the value obtained as a linear combination of elastic constants (B_{EOS} and B, respectively, in Table III). It appears that the experimental estimate of the C_{12} constant is significantly in error, while the two other components of the elastic tensor are much more accurate. The results of the PBE calculation agree very well with the PW91 results, while RPBE gives a 7% smaller C_{11} constant than the other two GGA functionals.

The band structure and density of states obtained using RPBE is shown in Fig. 2. The results obtained with various GGA functionals cannot be distinguished on the scale used here. These plots are qualitatively the same as in Refs. 1 and 11. The lowest states in the valence band are due to N 2*s* electrons. The next fully occupied set of bands is composed of hybridized Ti 3*d* and N 2*p* states. Metallic properties of titanium nitride are determined by Ti 3*d* states that dominate at E_F.

2. Surface energies

We studied TiN surfaces by constructing a supercell containing a few layers of TiN and a sufficiently large vacuum space. The standard method for extracting the surface energy from slab calculations is to subtract the bulk energy from the total energy of a slab when the number of layers approaches infinity:

$$S=\lim_{N\to\infty}\frac{1}{2}(E^N_{slab}-NE_{bulk}), \tag{2.2}$$

where E^N_{slab} is the total energy of the slab with N atoms and E_{bulk} is the bulk total energy per atom. In practice the limit is approximated by the Nth term. The factor 1/2 is due to the presence of two surfaces in the slab. The problem with such calculations is that the surface energy is very sensitive to the bulk energy.[41] Fiorentini and Methfessel suggested a rapidly converging method for calculating surface energies that does not require a separate energy evaluation for the bulk.[42] When N becomes large and convergence is approached, the slab energy is a linear function of N:

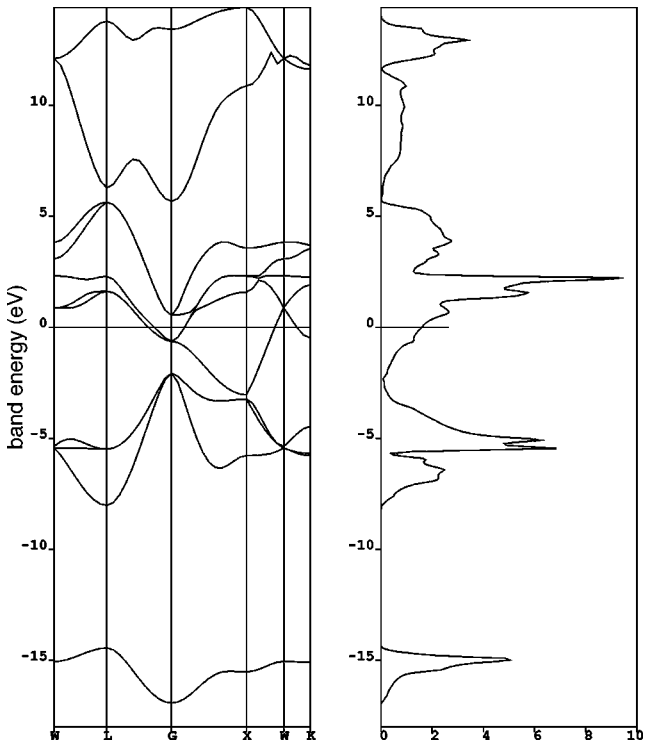

FIG. 2. Calculated band structure and density of states of TiN.

$$E^N_{slab}\approx 2S+NE_{bulk}. \tag{2.3}$$

One can fit a straight line to the E^N_{slab} as a function of N and extract the effective bulk energy from the slope. The surface energy is then obtained by replacing the bulk energy with that slope at Eq. (2.2).

We studied three surfaces of TiN, (100), (110), and (111), and calculated slab energies with three different thicknesses. For the (100) and (110) surfaces we calculated slab total energies for three, five, and seven layers. Since TiN occurs in the NaCl structure, the (111) surface has a single species termination, i.e., the surface is either Ti or N terminated. The odd number of layers in the slab supercell for the (111) orientation would result in an excess of titanium or nitrogen atoms depending on which species occupies the surface. When the stoichiometry is broken we cannot define the corresponding chemical potential (bulk energy), and surface energies cannot be calculated. We circumvented this problem by considering an even number of layers, so that the supercell contains one surface terminated by titanium and one surface terminated by nitrogen. This calculation gives the surface energy averaged between the two different terminations of the (111) surface. In this case we used slabs containing four, six, and eight atomic layers.

We used the smallest possible surface cell and 12 Å vacuum width in all slab calculations. The kinetic energy cutoff was set to 350 eV for all surfaces and slab thicknesses. The symmetrized k-point sets with Monkhorst-Pack parameters of $4\times4\times1$, $3\times4\times1$ and $4\times4\times2$ were used for the

TABLE IV. Calculated TiN surface energies (J/m^2) for relaxed and unrelaxed geometries.

	Relaxed			Static		
	RPBE	PBE	PW91	RPBE	PBE	PW91
S_{100}	1.06	1.28	1.30	1.53	1.75	1.76
S_{110}	2.59	2.85	2.86	2.87	3.13	3.14
S_{111}	4.59	4.92	4.95	5.08	5.42	5.45

(100), (110), and (111) surfaces, respectively. The surface energies were calculated by either keeping atoms in their ideal bulk positions (''static'' energy) or by allowing all atoms to relax with the exception of the central layer [or two central layers in the (111) case] (''relaxed'' energy). The lattice constant was always fixed at the equilibrium bulk value obtained with the relevant GGA functional as given in Table I. The bulk energies were obtained by fitting a straight line to the $E(N)$ dependence. The averages of the surface energies obtained from the five- and seven-layer calculations for the (100) and (110) surfaces and from the six- and eight-layer calculations for the (111) surface are given in Table IV for both static and relaxed configurations. We have checked the convergence of the surface energies with respect to the number of layers by repeating the RPBE calculation for the (100) surface using nine layers. The results for five, seven, and nine layers give 1.067, 1.057, and 1.077 J/m^2 respectively, which means that the calculations are converged to about 0.01 J/m^2

It is clear from Table IV that the PW91 calculations always gave the highest surface energy and RPBE the lowest. The differences were small between PW91 and PBE, while RPBE gave noticeably smaller, by about 0.2–0.3 J/m^2, values than PW91 and PBE. This trend persisted both in static and relaxed calculations for all three surface orientations. The greatest differences between the GGA functionals were observed for the (111) surface.

Although different GGA functionals resulted in slightly different values for surface energies, the energy differences between different surface orientations calculated within the same GGA formulation were consistent. The (100) surface has clearly the lowest surface energy with an $\sim$1.6 J/m^2 difference with respect to the (110) surface. The (110) surface was more stable in comparison to (111) by approximately 2.0 J/m^2.

Previous estimates of the surface energies for TiN were based on empirical arguments of bond breaking. Metallic bonding in TiN does not lend itself easily to such a mechanistic approach, as is illustrated by the following comparison. The estimates based on the sublimation energy have given 4.94, 6.99, and 8.53 J/m^2 for S_{100}, S_{110}, and S_{111}, respectively.[8] A similar estimate based on a slightly different bond-counting scheme gave 2.3, 2.6, and 4.0 J/m^2 for the same surfaces.[4] Interestingly, the second of these data sets is qualitatively similar to the relaxed RPBE values for the (110) and (111) surfaces (Table IV). However, both of these estimates fail to reproduce the actual ratios of surface energies. We obtained $S_{100}:S_{110}:S_{111}=1:2.44:4.33$, i.e., the (100) surface is significantly more stable. Empirical estimates give either 1:1.41:1.73 (Ref.8) or 1:1.13:1.73 (Ref.4), in both cases giving much less pronounced difference between the three orientations. In fact, surface relaxations contribute significantly to the error of the bond-breaking estimate. The static surface energies presented in Table IV exhibit the ratios that are closer to the empirical estimates, namely 1:1.87:3.32.

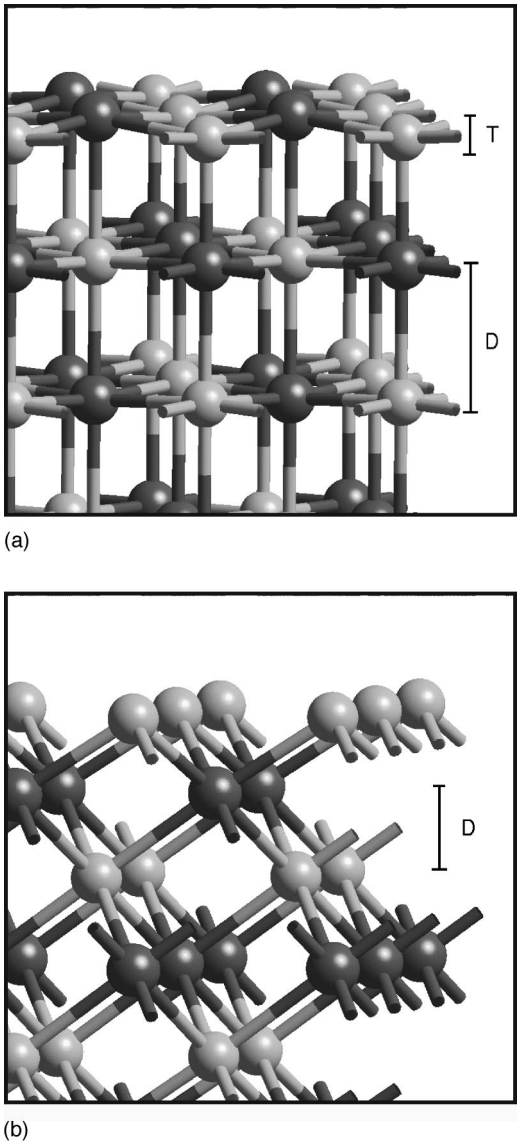

FIG. 3. Structural relaxations on the (a) (100) and (b) (111) surfaces of TiN (light and dark spheres represent titanium and nitrogen atoms, respectively). T is the plane width and D is the distance between the atomic planes.

3. Surface relaxations

In order to study the details of the surface relaxation we allowed five atomic layers to relax and kept two layers at the bottom of the surface fixed. The width of the vacuum layer was again fixed to 12 Å. The relative surface relaxations were found to be almost identical independent of the GGA functional used. We report RPBE distances that are slightly larger than the corresponding PW91 and PBE distances due to the larger lattice constant. We found that when a plane contains two atomic species, then in addition to the inward relaxation of the whole plane, the titanium atoms go further inside the surface than the nitrogen atoms [Fig. 3(a)]. In the

TABLE V. Relaxations of the (100), (110), and (111) surfaces of TiN. All values are in Å.

	(100)		(110)		(111)-Ti	(111)-N
	T	*D*	*T*	*D*	*D*	*D*
1	0.179	2.086	0.146	1.355	1.106	0.754
2	0.028	2.128	0.068	1.558	1.238	1.555
3	0.029	2.139	0.025	1.526	1.269	1.125
4	0.006	2.130	0.029	1.518	1.282	1.187
Bulk	0.0	2.130	0.0	1.506	1.229	1.229

case of the (111) orientation the N-terminated surface relaxes inwards more strongly than the Ti-terminated surface.

The structure of corrugated (100) and (110) surfaces can be described using two parameters. The plane width *T* for the planes that contain both Ti and N atoms is defined as a distance between the subplanes occupied by Ti and N atoms. This parameter goes to zero in the bulk and describes the degree of rumpling that occurs on the surface. The second parameter *D* represents the distance between the average positions of TiN planes parallel to the surface. We defined these positions simply as a mean value of the height of Ti and N subplanes. In the case of the (111) surface the distance *D* is the actual, not the averaged, subplane distance, since the surface planes are occupied only with either titanium or nitrogen atoms and the relaxations in the plane do not occur. The relaxation parameters for the (100), (110), Ti-terminated (111), and N-terminated (111) surfaces are given in Table V.

The values of *D* in the first row of Table V refer to the distance between the outermost and the second surface layer. The values of *T* in the first row of the table show the plane width at the outermost layer. The second value of *D* measures the distance between the second and the third layer from the surface and *T* is the plane width of the second layer, and so on.

As the number of layers increases, the parameter *D* far from the surface should approach the bulk value, i.e., *T* should go to zero and *D* to the corresponding distance in bulk. The convergence was reached for the (100) surface since the value of *T* was almost zero for the fourth layer, and the averaged distance between the planes was already equal to the bulk distance. The (110) surface showed a similar trend, but it was not as well converged. For the (111) surface it would have been necessary to study more layers to achieve a complete convergence, but the number of layers was sufficient to draw quantitative conclusions about the surface relaxations.

The data presented in Table V show the picture of the oscillating expansion and contractions of subsurface layers. The (100) surface shows the smallest oscillations: the top layer is contracted by 2.1%, and expansion (i.e., the *D* value is greater than the bulk value) observed in the third layer is only -0.4%. Such small values are typical for close-packed metallic surfaces.[43] The (110) surface is more open, which explains a large inward relaxation of the top plane, by 10%, and a bigger amplitude of oscillation: the second layer is relaxed upwards by 3.5%. The highest relaxations were observed on the N-terminated (111) surface, where the change in interatomic distances between the surface and subsurface atomic planes was found to be -39%.

D. Adsorption and diffusion of atomic hydrogen on the TiN(100) surface

Titanium nitride CVD growth techniques as outlined in the Introduction involve the use of Ti-containing molecules, e.g., TiI_4 or $TiCl_4$, and ammonia (NH_3), sometimes in the presence of other reaction constituents. A number of fundamental values pertinent to the gas-phase reactivity as well as to the molecule-surface interactions are necessary to model this process. The basic data required include adsorption energies and diffusion barriers and pathways for the reagents and reaction products. Atomic hydrogen is released during some of the reactions, and we start the study of fragments on the (100) surface of TiN by investigating adsorption and diffusion of hydrogen. The (100) surface of TiN has the lowest surface energy and plays the most important role in the CVD growth process, even for a polycrystalline film.[3]

The first set of results was obtained as follows. The hydrogen atom was placed on top of the TiN(100) surface and the energy minimum was searched for by letting hydrogen move on the rigid TiN surface. The surface was modeled with four layers where the lowest lying plane described the bulk and the three uppermost layers were fixed in the structure obtained from the seven-layer surface energy calculations. The (2×2) surface cell was used in order to minimize the interactions between hydrogens in the neighboring supercells. The distance between hydrogens in the neighboring cells was 6.025 Å in the RPBE calculations, which is sufficient to achieve convergence with respect to the lateral size of the unit cell. Two Monkhorst-Pack *k* points and the kinetic energy cutoff of 380 eV were used in all adsorption studies. The global minimum of the total energy was always found on top of the titanium atom with the Ti-H distance of 1.82 Å and 1.81 Å for RPBE and PW91, respectively.

The chemisorption energy of an adsorbate on the surface is calculated as the energy difference:

$$E_{chem}=E_{AM}-E_M-E_A, \tag{2.4}$$

where E_{AM} is the total energy of the combined system of adsorbate and metal surface, E_M and E_A are the energies of isolated surface and adsorbate, respectively. These calculations give the chemisorption energies of the hydrogen atom on the TiN(100) surface as -2.50 eV and -2.55 eV for RPBE and PW91 functionals, respectively. Although RPBE has been reported to give significantly improved chemisorption energies in the study of Ref. 19, the difference between PW91 and RPBE results is not significant in the present study.

The energy surface for H on a rigid TiN(100) surface was mapped out by calculating the energy of the system for different (x,y) positions of the hydrogen atom while letting hydrogen relax in the *z* direction. The calculations were performed in the irreducible surface area on the 21-point equidistant mesh with the 0.3 Å distance between the mesh points. The energy surface revealed a very simple structure. There is a second local minimum on a nitrogen atom that is about 0.2 eV higher in energy than the binding site on titanium, i.e., the binding energy was -2.31 eV. The bond length on this site was significantly shorter in comparison to the binding site on titanium with the 1.04 Å distance between nitrogen and hydrogen atoms.

The lowest-energy diffusion path connects the neighboring titanium atoms. It is a straight line across the saddle point located midway between the Ti atoms, and it has a diffusion barrier of 0.73 eV. Another low-energy path goes straight from the global minimum on titanium to the local minimum on nitrogen, and it has a comparable barrier of 0.76 eV. The barriers are close in energy, but the height of hydrogen on the surface changes strongly along the Ti-N-Ti path. On the Ti-Ti path the height changes by only 0.1 Å during the diffusion, but when the hydrogen diffuses from titanium to nitrogen the height changes by 0.7 Å as a consequence of the drastically different N-H and Ti-H bond lengths. This result suggests that the Ti-Ti path with an energy barrier of 0.73 eV represents the main diffusion mechanism for both thermodynamic and kinetic reasons.

The approximation of a rigid surface causes forces on the surface atoms when the hydrogen atom is allowed to relax. We performed further calculations by allowing both the first layer of the surface and the hydrogen to relax to the minimum-energy configuration. The chemisorption energy was slightly lowered and the titanium atom bonded to hydrogen raised towards hydrogen, shortening the bond length by 0.05 Å to 1.77 Å. The net result of the surface modification was to make the surface corrugations smaller. This might indicate that the surface relaxations vanish when the surface is covered by adsorbates. Although hydrogen adatom causes forces on the surface atoms, it is questionable whether heavy surface atoms have time to relax when hydrogen diffuses on the surface. It is likely that the rigid-surface calculations paint a more realistic picture of the energy surface for hydrogen than the fully relaxed calculations.

The final calculation was performed in the fully relaxed geometry. The cell contained seven TiN layers, and the two bottom layers were fixed to the bulk positions. This is the same layout as was used in the Sec. II C 3, but with (2×2) surface unit cell. The use of a bigger unit cell (57 atoms) and the need for full geometry optimization make these calculations more expensive than the ones described above. We have not attempted the full-potential energy surface calculation in this approach, but just obtained the binding energies for the two adsorption sites using RPBE and PW91 functionals.

The relaxation of the surface, as expected, increases the binding energy on both sites. The global minimum on Ti now has the energy of -2.88 eV, and the minimum on the N-site has the energy of -2.77 eV. The difference between these two sites becomes smaller as a result of the surface relaxation, i.e., 0.11 eV instead of the 0.19 eV on the rigid surface. The bond length Ti-H is 1.76 Å, very close to the result obtained with just one relaxed layer in a smaller supercell. The N-H bond length of 1.04 Å is not affected by the relaxation of the surface. This bond length is close to the value of 1.033 Å, the average distance between H and highly coordinated N in crystalline organic compounds.[38] The typical N-H bond length in the gas phase averaged over a number of small molecules[38] is 1.02 Å, and the calculated N-H bond length on the surface of TiN is expected to be longer than that.

The adsorbate-induced relaxation of the surface was found to be large and long-ranging. The Ti-site adsorption changed the sign of the plane width (see Table V) in the third layer, and changed the interplanar distances up to the fifth layer. Adsorption on the N site is characterized by increased surface corrugation, with the Ti-N height difference being nearly doubled. These findings are in contrast with the calculations for H on Pd and Re surfaces[43] where very little relaxation was found. The energetics of the hydrogen adsorption is, however, very similar. The values of -2.66 eV for the Pd(111) and -2.82 eV for the Re(0001) surfaces[43] are very close to the -2.88 eV reported here for the binding energy at the TiN(100) surface.

Finally, the same calculations were performed using the PW91 functional. We found the same two binding sites as with the RPBE functional. The global minimum on Ti atom is characterized by the adsorption energy of -2.99 eV, and the N site has the binding energy of -2.88 eV. The effect of using RPBE instead of the PW91 functional is thus small, not more than 0.1 eV in the chemisorption energy. The same magnitude of energy differences between PW91 and RPBE results was found in the study of H_2 dissociation on TiN. Even the effect of the form of the GGA functional on the surface energy alone was found to be higher than that. Apparently the competing effects of a larger cell parameter and of a different description of the exchange-correlation effects cancel to a great degree in the PW91 and RPBE calculations described above. If this is the case, the large effects seen previously for the RPBE calculations compared to the PW91 ones[19,22] could be an artifact of using inconsistent lattice parameters.

E. Adsorption and diffusion of molecular hydrogen on TiN(100) surface

In this section we report preliminary results of the study of H_2 adsorption on the (100) surface of titanium nitride. Our main interest in this case is to compare the results of RPBE and PW91 calculations rather than to give a complete study of the adsorption process.

The hydrogen molecule is known to dissociate on metallic surfaces, and there is a large body of *ab initio* studies of this dissociative adsorption. It has been shown that there is a small or no barrier for dissociation on Cu(100) (Ref. 44), W(100) (Ref. 45), Pd(100) (Ref. 46) or Rh(100) (Ref. 47) surfaces, while Ag(100) surface has a barrier for the H_2 dissociation.[47] This difference in the dissociation process can be explained by the higher chemical activity of the transition metals compared to the noble metal silver. One would expect then that the dissociation on the TiN surface should proceed without a barrier since it has even higher chemical activity.

We carried out only a very limited study of the interaction between H_2 and the (100) surface of TiN using two exchange-correlation functionals, PW91 and RPBE. We have attempted to optimize the geometry of the H_2 molecule that was placed on top of Ti and N atoms at approximately the same height as was found for the adsorption sites for atomic hydrogen. This procedure gives less information about the dissociation process than the calculation of the potential energy surface,[44–47] but it is a useful step in the search for molecular precursor states on the surface.

We found that the Ti site is likely to have a barrier for the H_2 dissociation since the geometry optimization procedure resulted in the molecule being removed from the surface in-

tact. The bond length of the product is 0.755 Å at the height of roughly 2.4 Å, which is consistent with the description of a free H_2 molecule above the transition metal surface.[44–47] The result was independent of the GGA functional used.

An interesting process was observed when the molecule was placed horizontally on top of the nitrogen atom. This configuration was found to be hugely unfavorable in terms of energetics, and geometry optimization resulted in the formation of the N vacancy on the surface and of the free NH_2 molecule. The geometry of the created NH_2 fragment is characterized by the N-H bond length of 1.033 Å and the H-N-H angle of 100.6°, very similar to the experimental data of 1.024 Å and 103.3°.[38] The relative energies of the created configurations are very similar in the PW91 and RPBE calculations. RPBE results always describe H_2 + TiN(100) complexes as slightly more unstable than the PW91 calculations, but the magnitude of the difference is small, less than 0.1 eV. This conclusion is consistent with the results for atomic hydrogen, and further calculations for bigger molecular fragments are needed to clarify the issue of the relative merits of PW91 and RPBE functionals in the studies of surface processes.

III. DISCUSSION

A. GGA functionals

In summarizing the results of the GGA testing we can conclude that all three functionals describe the structural properties of crystals and molecules accurately. The functionals were generally in good agreement with each other, but RPBE systematically resulted in slightly greater interatomic distances than PBE or PW91. The difference between RPBE and other functionals was found to be larger in ionic crystals.

In titanium nitride all GGA functionals described structural parameters better than LDA. The results obtained with the PW91 and PBE functionals were in excellent agreement with the experimental values. Both LDA and PW91 results were in very good agreement with the earlier all-electron theoretical calculations.[11]

The trends previously reported[19] for the RPBE functional as compared to PW91 were confirmed in the study of surface energies and hydrogen chemisorption energy on TiN. Both the surface energy for all orientations studied and the hydrogen chemisorption energy on the (100) surface were smaller in the RPBE calculations than in the PW91 calculations. However, the difference was not as significant as in Refs. 19 and 22, which could be due to the fact that we used consistent lattice parameters. In this study the difference between PW91 and RPBE in chemisorption energies was 0.1 eV while in Refs. 19 and 22 it was of the order of 0.5 eV for O, CO, N_2, and NO, on Rh, Ni, Pt, and Pd surfaces. Further calculations for bigger molecules adsorbed on TiN are planned to elucidate the role of the adsorbate in the magnitude of the RPBE correction.

B. Properties of titanium nitride

We presented the first atomistic study of the surface structure and energetics of three TiN surfaces. Our results support the experimental conclusion that the (100) surface has the lowest and the (111) surface the highest surface energy. We showed that simple estimates of the surface energy based on the counting of broken bonds on the surface can at best give the right order of magnitude and the correct order of the surface energies. Such empirical predictions fail to reproduce the ratio of surface energies, primarily due to the complete neglect of complex structural relaxations on the surfaces.

The accurate estimates of surface energies should help in understanding of competing mechanisms of the growth of thin films with a preferred growth orientation. The actual film orientation is determined by an interplay between the surface energy and the surface strain contribution. The strain effects are well understood in terms of the film-substrate lattice mismatch, while the energy effects until now had no quantitative description.

The surfaces of TiN were found to exhibit complex relaxations. The magnitude of the interplanar relaxations appears to agree with the results of similar studies for transition metal surfaces. The corrugations that we found on the (100) and (110) surfaces should be typical for the surfaces of binary compounds, although we are not aware of any relevant experimental studies on TiN. These corrugations might have important consequences for such processes as adsorption and diffusion, since kinetic characteristics of various pathways might depend on the height of surface atoms interacting with adsorbates. It is important to note that the effects of surface relaxations are long ranging (see Table V). It appears that five relaxed layers are sufficient to describe the structure and energetics of the (100) surface. One might, however, consider using thicker slabs for the modeling of the surface processes on the (110) and especially on the (111) surface of TiN.

Finally, we presented the results of the first study of the hydrogen atom adsorption and diffusion on the (100) surface of TiN. We found two possible adsorption sites with the adsorption energies of -2.88 eV on top of a titanium atom and -2.77 eV on top of a nitrogen atom. These results obtained with the RPBE functional give a slightly (by about 0.1 eV) weaker binding of the hydrogen adatom to the surface than the calculations carried out with the PW91 functional.

The accurate description of the energetics of the hydrogen adsorption is much more sensitive to the effect of surface relaxation than to the particular choice of the exchange-correlation functional. The relaxations caused by the adatom contributed approximately 0.4 eV to the calculated adsorption energy, which is a significant amount especially taking into account the fact that hydrogen is the smallest possible adsorbed species. We expect that the relaxation effects, in terms of both energetics and structural changes, will be more pronounced for other adsorbates. The diffusion barrier estimate of 0.73 eV was obtained from the rigid surface calculations and it appears to be accurate to within 0.1 eV since the relative energies of the energy minima are much less sensitive to the adsorbate-induced relaxation than the absolute values.

We believe that the present study opens the way to *ab initio* modeling of fundamental processes relevant to the CVD growth of TiN thin films. There appears to be no reason for not using the new RPBE exchange-correlation functionals in a self-consistent manner, although further studies of bigger adsorbates are needed to make a systematic con-

clusion on the effect of the form of the GGA functional on the calculated chemisorption energy.

ACKNOWLEDGMENTS

We are grateful to David Bird, who kindly brought to our attention his version of CASTEP which contains the PBE functional, and to Anatoli Korkin, who introduced us to the subject of the TiN growth. Michele Warren's help in calculation of elastic constants is greatly appreciated. We would also like to thank Matti Alatalo and Risto Nieminen for a critical reading of the manuscript. M.M. wishes to thank Molecular Simulations Inc. for cooperation and hospitality and Mike Payne and the Theory of Condensed Matter group of Cambridge University for their hospitality. The work of M.M. was supported by European Commission Leonardo da Vinci grant and Helsinki University of Technology training grant.

[1] K. Schwarz, CRC Crit. Rev. Solid State Mater. Sci. **13**, 211 (1987).
[2] J. B. Price, J. O. Borland, and S. Selbrede, Thin Solid Films **236**, 311 (1993).
[3] R. I. Hedge, R. W. Fiordalice, E. O. Travis, and P. J. Tobin, J. Vac. Sci. Technol. B **11**, 1287 (1993).
[4] J. Pelleg, L. Z. Zevin, S. Lungo, and N. Croitoru, Thin Solid Films **197**, 117 (1991).
[5] U. C. Oh and J. H. Je, J. Appl. Phys. **74**, 1692 (1993).
[6] J. H. Je, D. Y. Noh, H. K. Kim, and K. S. Liang, J. Appl. Phys. **81**, 6126 (1997).
[7] K. Min, S. Hofmann, and R. Shimizu, Thin Solid Films **295**, 1 (1997).
[8] J. P. Zhao, X. Wang, Z. Y. Chen, S. Q. Yang, T. S. Shi, and X. H. Liu, J. Phys. D **30**, 5 (1997).
[9] P. Blaha, J. Redinger, and K. Schwarz, Phys. Rev. B **31**, 2316 (1985).
[10] A. Dunand, H. D. Flack, and K. Yvon, Phys. Rev. B **31**, 2299 (1985).
[11] R. Ahuja, O. Eriksson, J. M. Wills, and B. Johansson, Phys. Rev. B **53**, 3072 (1996).
[12] L. Imhoff, A. Bouteville, and J. C. Remy, J. Electrochem. Soc. **145**, 1672 (1998).
[13] M. Ritala, M. Leskelä, E. Rauhala, and J. Jokinen, J. Electrochem. Soc. **145**, 2914 (1998).
[14] C. R. Kleijn, K. J. Kuijlaars, M. Okkerse, H. van Santen, and H. E. A. van den Akker, J. Phys. IV **9**, 117 (1999).
[15] H. Komiyama, Y. Shimogaki, and Y. Egashira, Chem. Eng. Sci. **54**, 1941 (1999).
[16] M. C. Payne, M. P. Teter, D. C. Allan, T. A. Arias, and J. D. Johannopoulos, Rev. Mod. Phys. **64**, 1045 (1992).
[17] J. P. Perdew, J. A. Chevary, S. H. Vosko, K. A. Jackson, M. R. Pederson, D. J. Singh, and C. Fiolhais, Phys. Rev. B **46**, 6671 (1992).
[18] J. P. Perdew, K. Burke, and M. Ernzerhof, Phys. Rev. Lett. **77**, 3865 (1996).
[19] B. Hammer, L. B. Hansen, and J. K. Nørskov, Phys. Rev. B **59**, 7413 (1999).
[20] H. T. Lorensen, J. K. Nørskov, and K. W. Jacobsen, Phys. Rev. B **60**, 5149 (1999).
[21] S. Dahl, A. Logadottir, R. C. Egeberg, J. H. Larsen, I. Chorkendorff, E. Tornqvist, and J. K. Nørskov, Phys. Rev. Lett. **83**, 1814 (1999).
[22] C. E. Tripa, T. S. Zubkov, J. T. Yates, M. Mavrikakis, and J. K. Nørskov, J. Chem. Phys. **111**, 8651 (1999).
[23] CASTEP Users Guide (Molecular Simulations Inc., San Diego, CA, 1998).
[24] D. Vanderbilt, Phys. Rev. B **41**, 7892 (1990).
[25] G. Kresse and J. Hafner, J. Phys.: Condens. Matter **6**, 8245 (1994).
[26] F. Birch, J. Geophys. Res. **83**, 1257 (1978).
[27] N. W. Ashcroft and N. D. Mermin, *Solid State Physics* (Saunders College, Philadelphia, 1976).
[28] G. N. Kamm and G. A. Alers, J. Appl. Phys. **35**, 327 (1964).
[29] A. V. Utkin, G. I. Kanel, S. V. Razorenov, A. A. Bogatch, and D. E. Grady, in *Proceedings of the Conference of the APS Topical Group on Shock Compression of Condensed Matter*, edited by S. C. Schmidt, D. P. Danekar, and J. P. Forbes (AIP Press, Woodbury, NY, 1998), p. 443.
[30] N. Schoenberg, Acta Chem. Scand. **8**, 213 (1954).
[31] V. A. Gubanov, A. L. Ivanovsky, and V. P. Zhukov, *Electronic Structure of Refractory Carbides and Nitrides* (Cambridge University Press, Cambridge, 1994).
[32] H. B. Huntington, Solid State Phys. **7**, 214 (1958).
[33] H. J. McSkimmin and P. Andreatch, J. Appl. Phys. **43**, 2944 (1972).
[34] S. V. Sinogeikin and J. D. Bass, Phys. Rev. B **59**, 14 141 (1999).
[35] H. E. Swanson and S. Fuyat, *Standard x-ray diffraction powder patterns*, Natl. Bur. Stand. Circ. No. 539 (U.S. GPO, Washington, D.C. 1953), Vol. 2, p. 41.
[36] C. Smith and L. Cain, J. Phys. Chem. Solids **36**, 205 (1975).
[37] R. Roberts and C. Smith, J. Phys. Chem. Solids **31**, 619 (1970).
[38] *CRC Handbook of Chemistry and Physics*, 73rd ed., edited by D. R. Lide (CRC Press, Boca Raton, 1993).
[39] *Handbook of High Temperature Compounds: Properties, Production, Applications*, edited by T. Ya. Kosolapova (Hemisphere, New York, 1990).
[40] J. O. Kim, J. D. Achenbach, P. B. Mirkarimi, M. Shinn, and S. A. Barnett, J. Appl. Phys. **72**, 1805 (1992).
[41] J. C. Boettger, Phys. Rev. B **49**, 16 798 (1994).
[42] V. Fiorentini and M. Methfessel, J. Phys.: Condens. Matter **8**, 6525 (1996).
[43] V. Pallassana, M. Neurock, L. B. Hansen, B. Hammer, and J. K. Nørskov, Phys. Rev. B **60**, 6146 (1999).
[44] J. A. White, D. M. Bird, I. Stich, and M. C. Payne, Phys. Rev. Lett. **73**, 1404 (1994).
[45] J. A. White, D. M. Bird, and M. C. Payne, Phys. Rev. B **53**, 1667 (1996).
[46] S. Wilke and M. Scheffler, Phys. Rev. B **53**, 4926 (1996).
[47] A. Eichler, J. Hafner, A. Gross, and M. Scheffler, Phys. Rev. B **59**, 13 297 (1999).